Magic Monotone for Faithful Detection of Nonstabilizerness in Mixed States

Krzysztof Warmuz,[1] Ernest Dokudowiec,[2,1] Chandrashekar Radhakrishnan,[3] and Tim Byrnes[1,4,5,6,*]

[1]*New York University Shanghai, NYU-ECNU Institute of Physics at NYU Shanghai, 567 West Yangsi Road, Shanghai 200124, China*

[2]*Gonville & Caius College, University of Cambridge, Cambridge CB2 1TA, United Kingdom*

[3]*Department of Computer Science and Engineering, NYU Shanghai, 567 West Yangsi Road, Shanghai 200124, China*

[4]*State Key Laboratory of Precision Spectroscopy, School of Physical and Material Sciences, East China Normal University, Shanghai 200062, China*

[5]*Center for Quantum and Topological Systems (CQTS), NYUAD Research Institute, New York University Abu Dhabi, Abu Dhabi, United Arab Emirates*

[6]*Department of Physics, New York University, New York, New York 10003, USA*

(Received 27 September 2024; accepted 9 June 2025; published 2 July 2025)

We introduce a monotone to quantify the amount of nonstabilizerness in mixed quantum states. The monotone gives a necessary and sufficient criterion for detecting the presence of nonstabilizerness for both pure and mixed states. The monotone is based on determining the boundaries of the stabilizer polytope in the space of Pauli string expectation values. The boundaries can be described by a set of hyperplane inequations, where violation of any one of these gives a necessary and sufficient condition for nonstabilizerness. The monotone is constructed by finding the hyperplane with the maximum violation and is a type of Minkowski functional. We also introduce a faithful witness based on similar methods. The approach is more computationally efficient than existing faithful mixed state monotones such as robustness of magic due to the smaller number and discrete nature of the parameters to be optimized.

DOI: 10.1103/2s3j-t22p

Introduction—The Gottesmann-Knill theorem [1] is one of the seminal results in the field of quantum computation, and it states that any quantum circuit that only consists of Clifford gates can be simulated on a classical computer in polynomial time [2,3]. The reason for this remarkable result is that such quantum circuits, called stabilizer or Clifford circuits, have a special symmetry, where the output of the circuit can be only one of an enumerable number of stabilizer states. Stabilizer states are simultaneous eigenstates of Pauli strings, and using the fact that under Clifford transformations such Pauli strings transform into other Pauli strings, one may efficiently keep track of the evolution in the quantum circuit [4,5]. Equivalently, in the Heisenberg picture, the operator evolution greatly simplifies due to the lack of operator growth thanks to the nature of Clifford transformations [6,7]. Since such Clifford circuits can be efficiently evaluated on a quantum computer, it follows that for a quantum computer to perform a task that is intractable for a classical computer, it must be capable of non-Clifford operations or have nonstabilizer states available to it. Such nonstabilizer states and operations, also called magic states and gates, can be considered a resource to perform universal quantum computation [8–11].

A natural task in this context is then to detect and quantify the amount of nonstabilizerness in a given quantum state. Restricting our discussion only to qubit systems (as opposed to qudits), one of the best known definition is the robustness of magic (RoM), which gives a faithful criterion for the detection of nonstabilizerness for mixed states, and satisfies several properties that make it a monotone [11,12]. Relative entropy of magic [8], and Jensen-Shannon divergence of magic [13] are distance-based quantifiers that are faithful measures of magic for mixed states.

Several alternative faithful monotones including the dyadic negativity were proposed by Seddon, Regula, Campbell and coworkers [14]. The main drawback of all these methods are that in an exact calculation they are highly numerically intensive since they involve the number of stabilizer states, which grow superexponentially with the number of qubits. Other quantities tend to be easier to calculate but have other drawbacks. The stablizer extent [15–17], stabilizer nullity, dyadic monotone [18], stabilizer Rényi entropy [19–22], GKP magic [23], and Bell magic [24] are faithful only for pure states. Sum negativity, mana, and related measures like Thauma [8,9,25–27] have been successfully computed using Monte Carlo methods [28,29] but are not applicable for qubit systems. The stabilizer norm can be applied to both pure and mixed states, but gives only a sufficient criterion for nonstabilizerness (hence is unfaithful) and does not give a very sensitive criterion in many cases [11,30]. It is therefore desirable to obtain a quantifier for nonstabilizerness that is faithful for mixed states and more easily computable than existing quantifiers.

*Contact author: tim.byrnes@nyu.edu

In this Letter, we introduce a new monotone to detect and quantify the amount of nonstabilizerness in a given state. Our approach is based upon determining the boundaries of the stabilizer polytope, which is the set of states that can be formed by a probabilistic combination of stabilizer states. By giving an explicit criterion for the facet hyperplanes in the space of Pauli string expectation values, we give necessary and sufficient conditions for a magic state. This can be formed into a monotone which quantifies the amount of nonstabilizerness. We also introduce a witness which is convenient for numerical computation and show their effectiveness in detecting nonstabilizerness for mixed states. The main advantage of our approach is that it is applicable for mixed states, in comparison to many quantifiers which are only faithful for pure states (see Supplemental Material [SM] [31]). We find that our monotone is easier to evaluate than other faithful mixed state monotones, and thus it constitutes a computationally viable alternative to quantifiers such as RoM.

Stabilizer states and quantifying nonstabilizerness—Consider an N-qubit system and denote the pure stabilizer states as $|S_i\rangle$, which are simultaneous eigenstates of 2^N commuting Pauli strings taking the form $P_k = \otimes_{n=1}^{N} P_n^{(l)}$, where $P_n^{(l)} \in \{I_n, X_n, Y_n, Z_n\}$ are Pauli matrices on site n with $l \in [0, 3]$. We order the Pauli strings according to the digits of $k \in [0, D^2 - 1]$ in base 4, such that $P_0 = I^{\otimes N}$, where $D = 2^N$ is the Hilbert space dimension. There are a total of $D_S = 2^N \prod_{n=1}^{N} (2^n + 1) \sim 2^{N^2/2}$ pure stabilizer states, so that the label runs from $i \in [1, D_S]$ [32]. More generally, stabilizer states can be formed by a probabilistic mixture of pure stabilizer states

$$\rho_S = \sum_{i=1}^{D_S} p_i |S_i\rangle\langle S_i|, \tag{1}$$

where $0 \le p_i \le 1$ are probabilities with $\sum_{i=1}^{D_S} p_i = 1$. The set of stabilizer states is known as the stabilizer polytope and consists of the convex hull of the pure stabilizer states.

A nonstabilizer state can be defined as any state that cannot be written in the form (1). By allowing p_i to take negative values, it becomes possible to write any arbitrary state ρ as an affine mixture of pure stabilizer states. Using this, a suitable quantifier for the nonstabilizerness of a general state is the robustness of magic (RoM), defined as

$$R(\rho) = \min \left\{ \sum_{i=1}^{D_S} |x_i| : \rho = \sum_{i=1}^{D_S} x_i |S_i\rangle\langle S_i| \right\}. \tag{2}$$

Here, the minimization is performed over the real parameters x_i, which may be negative in this case. A necessary and sufficient criterion for presence of nonstabilizerness is $R(\rho) > 1$, and all stabilizer mixtures (1) have $R(\rho) = 1$. Due to the superexponential number of such parameters typically this is a highly intensive numerical problem such that the largest system that can be calculated is $N \sim 5$ [11].

Another witness for nonstabilizerness is the stabilizer norm, defined as [11,30]

$$\|\rho\|_{\mathrm{st}} = \frac{1}{2^N} \sum_{k=0}^{D^2-1} |\langle P_k \rangle_\rho|, \tag{3}$$

where $\langle P_k \rangle_\rho = \mathrm{Tr}(\rho P_k)$, and detects nonstabilizerness when $\|\rho\|_{\mathrm{st}} > 1$. For $N = 1$, this is a necessary and sufficient criterion for nonstabilizerness and recovers the well-known octahedral stabilizer polytope which gives the boundary between magic and stabilizer states:

$$|\langle X \rangle| + |\langle Y \rangle| + |\langle Z \rangle| = 1. \tag{4}$$

For $N \ge 2$, the stabilizer norm is, however, only a sufficient condition, and some magic states are missed.

Polytope boundaries—We now formulate a general method to find stabilizer polytope boundaries, with the aim of generalizing the result (4) to arbitrary N. First let us discuss the space which the polytope exists in. We shall work in the space $\mathcal{P}$ defined by the expectation values of Pauli strings, such that any state ρ is represented by a vector of length D^2,

$$\langle \vec{P} \rangle_\rho = (\langle P_0 \rangle_\rho, \langle P_1 \rangle_\rho, \ldots, \langle P_{D^2-1} \rangle_\rho), \tag{5}$$

where $\vec{P}$ denotes a vector formed by all the Pauli string operators (with $+1$ coefficients). The vector $\langle \vec{P} \rangle_\rho$ contains full information of the density matrix ρ and naturally generalizes the space which the Bloch sphere exists in for $N = 1$.

The pure stabilizer states in $\mathcal{P}$ space, defined as $\vec{S}_i = \langle S_i | \vec{P} | S_i \rangle$, take a characteristic form of having D nonzero elements each taking a value of ± 1 and the remaining being zero (see [SM] [31]). The nonzero elements correspond to D mutually commuting Pauli strings, including the identity. A general mixed stabilizer state (1) in $\mathcal{P}$ space then forms a convex polytope parameterized by the region

$$\langle \vec{P} \rangle_{\rho_S} = \sum_{i=1}^{D_S} p_i \vec{S}_i, \tag{6}$$

where $0 \le p_i \le 1$. By extending p_i to negative values it is possible to write an arbitrary state as an affine mixture in the same way as done with RoM.

The boundary of the stabilizer polytope are formed by hyperplanes [33] that pass through a subset of stabilizer vectors $\vec{S}_i$ on a face of the polytope. The equation of a hyperplane is given by

$$\vec{a} \cdot \langle \vec{P} \rangle_\rho = b, \tag{7}$$

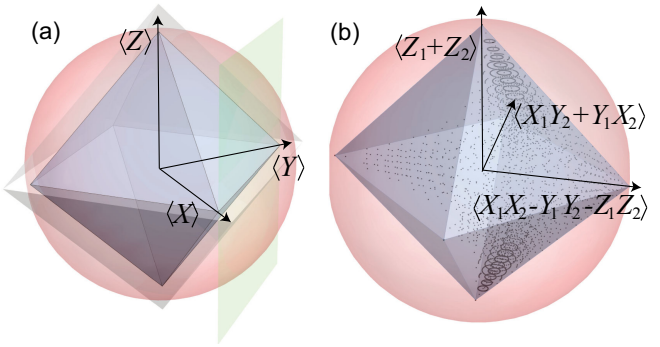

FIG. 1. Stabilizer polytope boundaries (10) according to various choices of $\vec{a}$. (a) The polytope boundaries for $N = 1$ corresponding to $\pm\langle X\rangle \pm' \langle Y\rangle \pm \pm'\langle Z\rangle \leq 1$, where $\pm, \pm'$ can be chosen independently (inner octahedron). Also shown is the polytope boundary $\langle X\rangle + \langle Y\rangle \leq 1$ (vertical plane). The surface of the outer octahedron defines planes of constant $\mathcal{M}(\rho) = 1.2$. The Bloch sphere showing the boundary of all states is also shown. (b) The polytope boundaries for $N = 2$ corresponding to $-3 \leq \langle X_1X_2 - Y_1Y_2 - Z_1Z_2\rangle \pm \langle X_1Y_2 + Y_1X_2\rangle \pm' \langle Z_1 + Z_2\rangle \leq 1$. The dots correspond to points with $\mathcal{W}(\rho) = 0$ for the Werner state $\rho = (1-\mu)I/D + \mu|\psi\rangle\langle\psi|$ with $|\psi\rangle = \cos(\theta/2)|00\rangle + e^{i\phi}\sin(\theta/2)|11\rangle$.

where $\vec{a}$ is a D^2 dimensional vector and b is a constant. The polytope boundaries must take a linear form (as opposed to, for instance, a curved surface), due to the linear mixture of the stabilizers along a boundary. Consider a particular face of the polytope consisting of a mixture of D_F stabilizers $F = \{|S_1^F\rangle, \ldots, |S_{D_F}^F\rangle\}$, which are a subset of all the stabilizers. Along a polytope boundary, we have the mixture

$$\rho_F = \sum_{j=1}^{D_F} p_j |S_j^F\rangle\langle S_j^F|. \tag{8}$$

Here $D_F < D_S$ such that some of the coefficients p_i have a zero value, giving the opportunity for them to turn negative. In $\mathcal{P}$ space, this appears as $\langle\vec{P}\rangle_{\rho_F} = \sum_{j=1}^{D_F} p_j \vec{S}_j^F$, which is a parametrized form of a hyperplane, equivalent to (7) for $\rho = \rho_F$.

The coefficients of the hyperplane must satisfy certain conditions in order that they form a valid boundary of the stabilizer polytope. We define a polytope boundary as any hyperplane that contains at least one point from the stabilizer polytope and defines the half-plane such that the polytope is on one side [see Fig. 1(a)]. Suppose we are given a particular $\vec{a}$ which defines the slope of the hyperplane. Then, if we take

$$b(\vec{a}) \equiv \max_{i\in[1,D_S]} \vec{a}\cdot\vec{S}_i, \tag{9}$$

this ensures that all mixed stabilizer states satisfy

$$\vec{a}\cdot\langle\vec{P}\rangle_{\rho_S} \leq b(\vec{a}). \tag{10}$$

Another bound can be obtained by replacing $\vec{a} \to -\vec{a}$, which corresponds to the lower bound of the polytope (see [SM] [31]).

Now suppose we start with a candidate subset F of all the pure stabilizers which form a mixture of the form (8), which may or may not lie on a polytope boundary. How do we determine whether F forms a polytope boundary? First find the equation of the hyperplane that runs through all the stabilizers in F by demanding that (see [SM] [31])

$$\vec{a}\cdot\left(\vec{S}_j^F - \vec{S}_1^F\right) = 0 \tag{11}$$

for all $j \in [2, D_F]$. Depending upon the number of stabilizers M chosen, this may result in an underconstrained or overconstrained set of equations. In the overconstrained case, there may be no solution to (11) as no hyperplane exists to go through all the stabilizers in F, meaning that F is not a polytope boundary. In the underconstrained case, this will result in a set of hyperplanes with free parameters. Once the coefficients that satisfy (11) are found, all $\vec{a}\cdot\vec{S}_j^F$ equal a constant b for all $j \in [1, D_F]$. Then to see whether this is a polytope boundary, we must verify that it satisfies (10), which can be equally written as

$$\vec{a}\cdot(\vec{S}_1^F - \vec{S}_i) \geq 0. \tag{12}$$

for all $i \in [1, D_S]$. This condition demands that the hyperplane runs on one side of the polytope such that all stabilizer points are lower than it. Thus if (11) and (12) can be satisfied, we can conclude that F forms a polytope boundary.

Polytope boundary symmetries—The stabilizer polytopes for multiqubit states possess several symmetries due to the properties of stabilizer states [34]. First, due to the fact that Clifford unitaries map a pure stabilizer state onto another pure stabilizer state $U_C|S_i\rangle \propto |S_{C(i)}\rangle$, a Clifford transformation of the states on the polytope boundary (8) gives another polytope boundary $U_C\rho_F U_C^\dagger$. Given that (10) is a polytope boundary, then the same inequation with $\vec{P} \to U_C\vec{P}U_C^\dagger$ is also a polytope boundary, which is a permutation of the Pauli strings up to sign changes. Another symmetry is due to the spin flip symmetry of individual qubits. Here we consider a spin flip to be along one of the stabilizer axes X, Y, Z. This consists of changing sign of one Pauli matrix on a site n, i.e., $P_n^{(l)} \to -P_n^{(l)}$ for $l \in [1, 3]$. In the Pauli vector $\vec{P}$, this will change the signs of 4^{N-1} of the P_n. Then, given that (10) is a polytope boundary, the same inequation with this transformation is also a polytope boundary. Multiple spin flips can be applied, in combination with Clifford transformations, which gives a family of hyperplanes which together define the boundary of the polytope (see [SM] [31]).

Another important simplification is that the hyperplane vector $\vec{a}$ only takes integer components $a_k \in \mathbb{Z}$. The reason

for this originates from the fact that the stabilizer vectors only have components that are $[\vec{S}_i]_k \in \{0, \pm 1\}$, such that any hyperplane running through them must also take coefficients that are integral (see [SM] [31]). This also implies that $b(\vec{a}) \in \mathbb{Z}$.

Example polytope boundaries—Figure 1 shows some example polytope boundaries determined by the above procedure. Figure 1(a) shows the familiar single qubit case. Choosing any three nonorthogonal stabilizers for F gives the 8 hyperplanes corresponding to the faces of the octahedral stabilizer polytope. Choosing two stabilizers (e.g. along the $\langle X \rangle$ and $\langle Y \rangle$ axis) defines a boundary only along one edge of the polytope, but nevertheless it is a valid polytope boundary. For $N = 2$ [Fig. 1(b)], we use a similar procedure to construct a subset F that corresponds to a fully constrained problem. This is performed by starting with a seed set of stabilizers which are in the vicinity of a state of interest, and then continue to add stabilizers until (11) and (12) are fully constrained. For the example shown, we find that 33 stabilizers fully constrain the hyperplane, each giving a solution of $\vec{a}$ with 7 Pauli strings with equal weight. An example of eight such hyperplanes is shown in Fig. 1(b), which forms part of the polytope boundary in the 16-dimensional space, in agreement with Ref. [35] obtained with alternative methods. It is noteworthy to add that for systems consisting of 2 or more qubits, the stabilizer polytope boundaries are given by several families of hyperplanes which are not related to one another by any of the Clifford symmetries. Plotting zero magic Werner states for the states $\cos(\theta/2)|00\rangle + e^{i\phi}\sin(\theta/2)|11\rangle$ we find that all fall within the hyperplanes. However, in the negative $\langle X_1X_2 - Y_1Y_2 - Z_1Z_2 \rangle$ direction, there are other polytope boundaries (not plotted), which is the reason that Werner state does not reach the edge of the octahedron.

Necessary and sufficient conditions—In deriving (11) and (12), we took the approach of deriving the polytope boundary that passes through a given subset of stabilizers F. In fact, it is not necessary to specify F to obtain a valid polytope boundary since given any $\vec{a}$, the bound may be evaluated by (9). The stabilizer polytope is then defined by the set of points in $\mathcal{P}$ space, which satisfies

$$SP_N = \left\{ \vec{a} \cdot \langle \vec{P} \rangle_\rho \leq b(\vec{a}), \quad \forall \vec{a} \in \mathbb{Z}^{D^2} \right\}. \tag{13}$$

A violation of (13) is then a necessary and sufficient condition for the detection of nonstabilizerness. This is a sufficient condition as already shown, since any stabilizer mixture must follow (10). It is also a necessary condition because no magic states can exist inside the stabilizer polytope (see [SM] [31]).

Magic monotone—Based on the above we can define the magic monotone,

$$\mathcal{M}(\rho) = \max_{\{\vec{a} \in \mathbb{Z}^{D^2}, a_0 = 0\}} \left[\frac{\vec{a} \cdot \langle \vec{P} \rangle_\rho}{b(\vec{a})} \right], \tag{14}$$

where the maximization is performed over all $\vec{a}$. Since $\langle P_0 \rangle = 1$ for any state, we may take $a_0 = 0$ leaving the remaining $D^2 - 1$ variables to be optimized. For $\vec{a} = \vec{0}$, we take the argument of the maximization to be 1, which guarantees that $\mathcal{M}(\rho) \geq 1$. The quantity to be maximized is (10), such that if there is any hyperplane which shows a violation, we will have $\mathcal{M}(\rho) > 1$. This is a necessary and sufficient criterion for nonstabilizerness when $\mathcal{M}(\rho) > 1$. The quantifier defined above possesses key properties that make it a valid monotone [36]: (1) $\mathcal{M}(\rho) \geq 1$; (2) invariance under Clifford unitaries $\mathcal{M}(\rho) = \mathcal{M}(U_C \rho U_C^\dagger)$; (3) faithfulness $\mathcal{M}(\rho) = 1$ iff $\rho = \rho_S$, otherwise $\mathcal{M}(\rho) > 1$; (4) monotonicity $\mathcal{M}(\mathcal{E}(\rho)) \leq \mathcal{M}(\rho)$, where $\mathcal{E}$ is a stabilizer channel; (5) convexity $\mathcal{M}(\sum_k p_k \rho_k) \leq \sum_k p_k \mathcal{M}(\rho_k)$ (see [SM] [31]).

The definition (14) shows how the magic states are distributed in $\mathcal{P}$-space. Consider the set of states with equal nonstabilizerness $\mathcal{M}(\rho) = r$. This defines a set of hyperplanes $\vec{a} \cdot \langle \vec{P} \rangle_\rho = r b(\vec{a})$, which corresponds to an enlarged polytope that has the same shape as the stabilizer polytope (Fig. 1(a)). The form of (14) is consistent with a Minkowski functional [37], which is a way of measuring the distance of a point from the stabilizer polytope by seeing how much the polytope has to be scaled up in order for it to just include the point. As a result, this measure inherits the same symmetries as the underlying stabilizer polytope.

An interesting point here is that this structure precludes alternative definitions of monotones based on, for instance, Euclidean distance of states in $\mathcal{P}$ space from the polytope. Such a measure would result in a polytope with rounded edges and corners when finding points with constant nonstabilizerness, which is inconsistent with points of constant RoM even for $N = 1$. It would also not be comparable without rescaling between points whose nearest hyperplanes belong to different families for multiqubit systems, due to Euclidean distance being spherically symmetric.

Numerical demonstration—We now show some explicit numerical examples using our methods to show its utility in a mixed state context. In addition to explicitly calculating $\mathcal{M}(\rho)$, we also use the necessary and sufficient conditions (13) to construct a faithful witness,

$$\mathcal{W}(\rho) = \max_{\{|a_k| \leq 1, a_0 = 0\}} \left[\vec{a} \cdot \langle \vec{P} \rangle_\rho - b(\vec{a}) \right], \tag{15}$$

which is a nonnegative, Clifford invariant, and faithful quantity. We note that it is stronger than conventional witnesses, which are not necessarily faithful. Here, we normalized the vector $\vec{a}$ such that all coefficients lie in the range $|a_k| \leq 1$ (see [SM] [31]). While this means that strictly a_k takes only rational values, numerically there is little benefit of this constraint and we treat a_k as a real

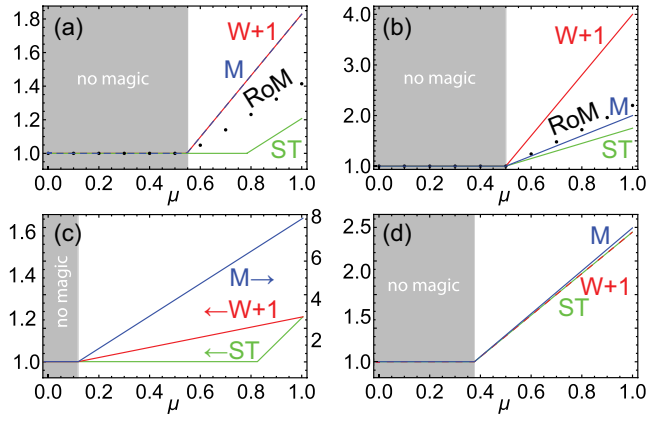

FIG. 2. Comparison of various magic quantifiers for various Werner states defined as $\rho = (1-\mu)I/D + \mu|\psi\rangle\langle\psi|$. Calculated are states (a) $|\psi\rangle = (|00\rangle + e^{i\pi/4}|11\rangle)/\sqrt{2}$; (b) $|\psi\rangle = (|00\rangle + |01\rangle + |10\rangle + i|11\rangle)/2$; (c) $|\psi\rangle = (|00000\rangle + e^{i\pi/4}|11111\rangle)/\sqrt{2}$; (d) $|\psi\rangle = (|0\rangle + e^{i\pi/4}|1\rangle)^{\otimes 5}/\sqrt{2^5}$. Lines shown are robustness of magic (RoM), stabilizer norm (ST), our magic monotone (14) (M), and magic witness (15) (W + 1). In (c) the arrows indicate the axes that are used for each quantity. For all plotted quantities a value greater than 1 indicates the presence of nonstabilizerness. The magic witness $\mathcal{W}(\rho)$ we have added 1 to (15). For the stabilizer norm we plot $\mathrm{ST} = \max(1, \|\rho\|_{\mathrm{st}})$.

parameter. We find that for the small scale systems as plotted here, the maximization for both $\mathcal{M}(\rho)$ and $\mathcal{W}(\rho)$ can be calculated within a few minutes with modest computational resources. Using heuristics to evaluate (9), we estimate that the typical complexity is approximately $O(4^N)$ (see [SM] [31]). This is much faster than evaluating RoM, which involves a nonlinear optimization over $D_S \sim 2^{N^2/2}$ real variables. While RoM is in principle a faithful measure of nonstabilizerness, the large computational overhead effectively can give false positives as a magic detector, due to the imperfect optimization giving a decomposition with negative coefficients.

Figure 2 shows a comparison of various quantifiers for various Werner states. We see that both our magic witness and monotone successfully detects nonstabilizerness in the same region as RoM for $N = 2$ [Figs. 2(a) and 2(b)] and gives consistent results for $N = 5$ [Figs. 2(c) and 2(d)]. Both of these quantities often shows an improvement in the detection range over the stabilizer norm, which is only a sufficient condition for nonstabilizerness. Examining the expression for the stabilizer norm (3), we can see that this is a particular case of our criterion where $\vec{a} = \mathrm{sgn}(\langle P_n \rangle)$ and $b(\vec{a}) = 2^N$. This would correspond to one particular choice of hyperplane, which may not correspond to the polytope boundary giving the tightest bound. By running over all polytope boundaries, our witness is able to detect magic states that are missed by the stabilizer norm.

Conclusions—We have introduced an approach to detect and quantify the amount of nonstabilizerness in an arbitrary quantum state by finding the hyperplane equations defining the stabilizer polytope. By testing all possible hyperplanes, one can obtain a necessary and sufficient criterion for detecting nonstabilizerness. This can be adapted into a magic monotone which quantifies the amount of nonstabilizerness according to the scale factor required to enlarge the polytope such that it falls on its boundary. We find that the approach works well numerically, where mixed magic states can be detected much more efficiently than other faithful mixed state monotones such as RoM. We note we have only compared RoM evaluations using conventional methods which are limited to $N \leq 5$ due to computational costs. Using more advanced methods RoM can be evaluated up to $N \leq 8$ [38]. There are numerous ways that this approach can be developed further, and thereby improving methods for magic detection. A better understanding of the polytope boundaries for a given N would allow one to further constrain the maximization in (14), to reduce the search space of the hyperplanes. Improvements in obtaining the bound $b(\vec{a})$, which in a brute force approach involves a discrete maximization over D_S, would lead to further improvements in efficiency, since the remaining optimization in (14) involves a smaller $D^2 - 1$ variables. By further developing these techniques it is likely that the nonstabilizerness in larger systems can be quantified more efficiently.

Acknowledgments—This work is supported by the SMEC Scientific Research Innovation Project (2023ZKZD55); the Science and Technology Commission of Shanghai Municipality (22ZR1444600); the NYU Shanghai Boost Fund; the China Foreign Experts Program (G2021013002L); the NYU-ECNU IInstitute of Physics at NYU Shanghai; the NYU Shanghai Major-Grants Seed Fund; and Tamkeen under the NYU Abu Dhabi Research Institute Grant No. CG008.

[1] D. Gottesman, International conference on group theoretic methods in physics, arXiv:quant-ph/9807006.
[2] S. Aaronson and D. Gottesman, Improved simulation of stabilizer circuits, Phys. Rev. A **70**, 052328 (2004).
[3] S. Anders and H. J. Briegel, Fast simulation of stabilizer circuits using a graph-state representation, Phys. Rev. A **73**, 022334 (2006).
[4] D. Gottesman, *Stabilizer Codes and Quantum Error Correction* (California Institute of Technology, Pasadena, 1997).
[5] M. A. Nielsen and I. Chuang, *Quantum Computation and Quantum Information* (Cambridge University Press, Cambridge, 2010).
[6] D. Aharonov, X. Gao, Z. Landau, Y. Liu, and U. Vazirani, A polynomial-time classical algorithm for noisy random circuit sampling, in *Proceedings of the 55th Annual ACM Symposium on Theory of Computing* (Association for Computing Machinery, New York, 2023), pp. 945–957.

[7] I. Ermakov, O. Lychkovskiy, and T. Byrnes, Unified framework for efficiently computable quantum circuits, arXiv:2401.08187.
[8] V. Veitch, S. H. Mousavian, D. Gottesman, and J. Emerson, The resource theory of stabilizer quantum computation, New J. Phys. **16**, 013009 (2014).
[9] V. Veitch, C. Ferrie, D. Gross, and J. Emerson, Negative quasi-probability as a resource for quantum computation, New J. Phys. **14**, 113011 (2012).
[10] A. Mari and J. Eisert, Positive Wigner functions render classical simulation of quantum computation efficient, Phys. Rev. Lett. **109**, 230503 (2012).
[11] M. Howard and E. Campbell, Application of a resource theory for magic states to fault-tolerant quantum computing, Phys. Rev. Lett. **118**, 090501 (2017).
[12] G. Vidal and R. Tarrach, Robustness of entanglement, Phys. Rev. A **59**, 141 (1999).
[13] P. Tian and Y. Sun, Quantifying magic resource via quantum Jensen–Shannon divergence, J. Phys. A **58**, 015303 (2024).
[14] J. R. Seddon, B. Regula, H. Pashayan, Y. Ouyang, and E. T. Campbell, Quantifying quantum speedups: Improved classical simulation from tighter magic monotones, PRX Quantum **2**, 010345 (2021).
[15] S. Bravyi and D. Gosset, Improved classical simulation of quantum circuits dominated by Clifford gates, Phys. Rev. Lett. **116**, 250501 (2016).
[16] S. Bravyi, G. Smith, and J. A. Smolin, Trading classical and quantum computational resources, Phys. Rev. X **6**, 021043 (2016).
[17] S. Bravyi, D. Browne, P. Calpin, E. Campbell, D. Gosset, and M. Howard, Simulation of quantum circuits by low-rank stabilizer decompositions, Quantum **3**, 181 (2019).
[18] M. Beverland, E. Campbell, M. Howard, and V. Kliuchnikov, Lower bounds on the non-Clifford resources for quantum computations, Quantum Sci. Technol. **5**, 035009 (2020).
[19] L. Leone, S. F. E. Oliviero, and A. Hamma, Stabilizer Rényi entropy, Phys. Rev. Lett. **128**, 050402 (2022).
[20] L. Leone and L. Bittel, Stabilizer entropies are monotones for magic-state resource theory, Phys. Rev. A **110**, L040403 (2024).
[21] T. Haug and L. Piroli, Stabilizer entropies and nonstabilizerness monotones, Quantum **7**, 1092 (2023).
[22] S. F. Oliviero, L. Leone, A. Hamma, and S. Lloyd, Measuring magic on a quantum processor, npj Quantum Inf. **8**, 148 (2022).
[23] O. Hahn, A. Ferraro, L. Hultquist, G. Ferrini, and L. García-Álvarez, Quantifying qubit magic resource with Gottesman-Kitaev-Preskill encoding, Phys. Rev. Lett. **128**, 210502 (2022).
[24] T. Haug and M. S. Kim, Scalable measures of magic resource for quantum computers, PRX Quantum **4**, 010301 (2023).
[25] X. Wang, M. M. Wilde, and Y. Su, Efficiently computable bounds for magic state distillation, Phys. Rev. Lett. **124**, 090505 (2020).
[26] X. Wang, M. M. Wilde, and Y. Su, Quantifying the magic of quantum channels, New J. Phys. **21**, 103002 (2019).
[27] N. Koukoulekidis and D. Jennings, Constraints on magic state protocols from the statistical mechanics of Wigner negativity, npj Quantum Inf. **8** (2022).
[28] H. Pashayan, J. J. Wallman, and S. D. Bartlett, Estimating outcome probabilities of quantum circuits using quasiprobabilities, Phys. Rev. Lett. **115**, 070501 (2015).
[29] D. A. Kulikov, V. I. Yashin, A. K. Fedorov, and E. O. Kiktenko, Minimizing the negativity of quantum circuits in overcomplete quasiprobability representations, Phys. Rev. A **109**, 012219 (2024).
[30] E. T. Campbell, Catalysis and activation of magic states in fault-tolerant architectures, Phys. Rev. A **83**, 032317 (2011).
[31] See Supplemental Material at http://link.aps.org/supplemental/10.1103/2s3j-t22p for the formal proof regarding $\vec{a}$ vector normalization see Supplementary Material.
[32] D. Gross, Hudson's theorem for finite-dimensional quantum systems, J. Math. Phys. (N.Y.) **47**, 122107 (2006).
[33] B. Grünbaum, V. Klee, M. A. Perles, and G. C. Shephard, *Convex Polytopes* (Springer, New York, 1967), Chap. 2.1.
[34] M. Heinrich and D. Gross, Robustness of magic and symmetries of the stabiliser polytope, Quantum **3**, 132 (2019).
[35] B. W. Reichardt, Quantum universality by state distillation, Quantum Inf. Comput. **9**, 1030 (2009).
[36] A. Streltsov, G. Adesso, and M. B. Plenio, Colloquium: Quantum coherence as a resource, Rev. Mod. Phys. **89**, 041003 (2017).
[37] L. Narici and E. Beckenstein, *Topological Vector Spaces* (Chapman and Hall/CRC, London, 2010), 2nd ed., pp. 192–193.
[38] H. Hamaguchi, K. Hamada, and N. Yoshioka, Handbook for quantifying robustness of magic, Quantum **8**, 1461 (2024).